Int J Clin Exp Med 2016;9(6):8925-8933
www.ijcem.com /ISSN:1940-5901/IJCEM0018400

Original Article

Reproductive performance and histological characteristics of select organs in NIH hairless mice

Jian Chen[1*], Bao Yuan[1*], Tuo Zhu[1], Yan Cai[2], Jin-Ping Hu[1], Yan Gao[1], Wei Gao[1], Hao Jiang[1], Wen-Zhi Ren[1], Jia-Bao Zhang[1]

[1]Department of Laboratory Animal Center, College of Animal Sciences, Jilin University, Changchun 130062, Jilin, China; [2]Department of Laboratory Animal Center, Changchun Institute of Biological Products Co., Ltd., Changchun 130062, Jilin, China. [*]Equal contributors.

Received August 11, 2015; Accepted May 10, 2016; Epub June 15, 2016; Published June 30, 2016

Abstract: Five pairs of two-month-old NIH hairless mice were mated, and five pairs of two-month-old NIH normal mice were mated as the control. The number of pups and the survival rate of the pups after weaning were recorded. Statistical methods were used to analyze the organ coefficients of the heart, liver, spleen, lung, and kidney for the one-month-old and two-month-old normal mice and NIH hairless mice (five males, five females). Paraffin sections of the heart, liver, lung, kidney, and skin for the one-month-old NIH hairless mice and normal mice were prepared and observed under a light microscope and the dorsal skin of the one-week-old and two-week-old NIH hairless mice and normal mice were observed using scanning electron microscopy (SEM). Our results showed that the litter size and the survival rate of the pups after weaning of the NIH hairless mice were lower than those of the normal mice, with significant differences in some of the organ coefficients ($P<0.05$); no significant differences were found in the histological characteristics of the heart, liver, lung and kidney tissue. Manifestations of the dorsal skin in the NIH hairless mice included a small number of hair follicles in the dermis and subcutaneous tissue, with keratosis in the follicles, while no significant hair shaft structure was observed.

Keywords: Litter size, survival rate of the pups after weaning, histology, NIH mice

Introduction

As mutations occurring under natural conditions, the use of spontaneous mutations is an important approach to obtain transgenic animal models [1]. Common spontaneous mutant mouse models include mutant mice with dwarfism, mice with muscular dystrophy, diabetic mice, obese mice, mice with bone sclerosis, mice with retinal degeneration, mice with asplenia, and nude mice, which are widely used in studies of drug development and pathogenesis [2-6].

This study primarily aimed to investigate select biological characteristics of NIH hairless mice created through a spontaneous gene mutation and obtain information regarding their reproductive performance and histology, thereby providing a research basis for the study of this mouse model with a mutation affecting the coat and hair.

Materials and methods

Ethics statement

The animal slaughter experiments were conducted in accordance with the guidelines of Jilin University on the Review of Welfare and Ethics of Laboratory Animals approved by the Jilin Province Administration Office of Laboratory Animals. All animal procedures were approved by Institutional Animal Care and Use Committee (IACUC) of Jilin University (Permit Number: 20140304). All surgery was performed under sodium pentobarbital anesthesia, and all efforts were made to minimize suffering.

Experimental animals and the feeding and rearing environment

SPF grade NIH hairless mice and normal mice were provided by the Changchun Institute of Biological Products Co., Ltd (SCXK-2011-003).

Table 1. Comparison of the litter size and survival rate of the pups after weaning of the NIH hairless mice and NIH normal mice

	Litter size	Survival rate
NIH hairless mice	8.8000±1.7889	73.8560%±12.1411%
NIH normal mice	12.0000±1.4142	91.9680%±8.2354%
P	0.015*	0.028*

Note: *indicates that the two sets of data were significantly different ($P<0.05$).

Sterile mouse feed and an IVC rearing system were provided by the Laboratory Animal Center of Jilin University (SYXK-2013-005).

Reagents and equipment

Formaldehyde solution (25%) and glutaraldehyde solution (25%) were purchased from Tianjin Fuchen Chemical Reagent Factory. Other reagents included eosin (AR), hematoxylin (AR), neutral balsam, absolute alcohol, and xylene. The electronic scale was purchased from METTLER TOLEDO. Sodium pentobarbital were purchased from Sigma. The EG1150H paraffin embedding station and RM2245 rotary microtome were purchased from LEICA. The ES-2030 Freeze Dryer, E-1010 Ion Sputter, and S3400N scanning electron microscope were purchased from Hitachi.

Breeding of NIH mice

Five pairs of two-month-old NIH hairless mice were mated, and five pairs of two-month-old normal mice were mated as the control. After the pups were born, the number of pups were recorded with routine observation and recording. After weaning, the pups were divided by gender, and the males and females were reared in separated cages with observation.

Sample collection

Five of each gender of one-month-old and two-month-old NIH hairless mice and NIH normal mice were weighed and sacrificed by cervical dislocation, followed by dissection and observation. The heart, liver, lungs, kidneys, and dorsal skin were collected and stored in 4% formaldehyde solution after drying the blood and removing the blood clots and fascia. The one-week-old and two-week-old NIH hairless pups and normal pups were sacrificed by cervical dislocation under sodium pentobarbital anesthesia, and the dorsal skin was collected and flattened on filter paper in 2.5% glutaraldehyde solution.

Analysis of the organ coefficients and histological observations of the organs and skin

The live mice were weighed, and the weights of the heart, liver, spleen, lung, kidney and thymus were routinely measured. Organ coefficient = organ weight/body weight of the mouse ×100%. The data are presented as means ± SEM. Differences were analyzed by the Student t test using SPSS 19, and $P<0.05$ was considered statistically significant.

The tissues of the heart, liver, lung, kidney, and skin from mice were fixed in 4% formaldehyde, embedded in paraffin, and sliced, and they were then observed under a light microscope after HE staining.

Scanning electron microscopy (SEM) of the dorsal skin

The dorsal skin was collected from the one-week-old and two-week-old NIH hairless mice and normal mice and fixed with 2.5% glutaraldehyde solution overnight at 4°C, then washed, trimmed and fixed. Next, the samples were rinsed, dried, dehydrated and coated with gold on the ion sputtering coating apparatus.

Results

Litter size and survival rate of the pups after weaning of the NIH hairless mice

The results of the statistical analysis showed that the litter size of the NIH hairless mice was smaller than that of the NIH normal mice; the survival rate of the pups after weaning of the NIH hairless mice was also lower than that of the NIH normal mice, with statistically significant differences (**Table 1**). The appearance of the one-month-old NIH hairless mice was significantly different from that of the normal mice. The backs of the NIH hairless mice were covered with fine hair, with folds in the neck skin, and the internal organs were observable through the skin. The NIH normal mice had thick and shiny coats, and the dorsal skin was not visible (**Figure 1**).

Organ coefficients and histological characteristics of select organs in the NIH hairless mice

The results of our statistical analysis showed that the average organ coefficients of the heart,

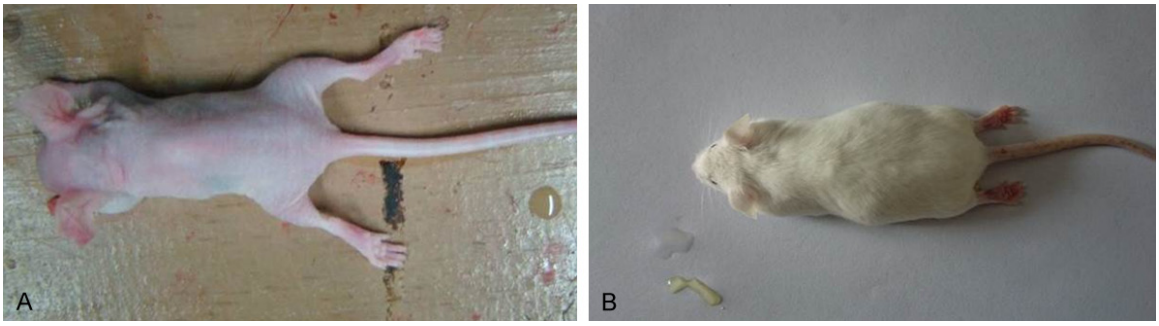

Figure 1. Appearance of the one-month-old mice. A: One-month-old NIH hairless mice; B: One-month-old NIH normal mice. The appearance of the NIH hairless mice was significantly different from that of the normal mice. The backs of the NIH hairless mice were only covered with fine hair, and the internal organs were observable through the skin.

Table 2. Comparison of the organ coefficients of the one-month-old mice

	Hairless mice (♂)	Normal mice (♂)	*P*	Hairless mice (♀)	Normal mice (♀)	*P*
Heart	0.005912±0.000469	0.004974±0.000863	0.075	0.006425±0.000750	0.004356±0.000414	0.000*
Liver	0.051862±0.004755	0.046982±0.005575	0.175	0.049193±0.001634	0.050932±0.003631	0.317
Spleen	0.007934±0.002523	0.005386±0.000833	0.064	0.004375±0.001353	0.00542±0.000993	0.186
Lung	0.011122±0.001909	0.007452±0.001279	0.007*	0.010643±0.001698	0.006944±0.001126	0.002*
Left kidney	0.008484±0.002173	0.006458±0.000530	0.077	0.011670±0.002184	0.006362±0.000743	0.001*
Right kidney	0.007440±0.001215	0.006940±0.000662	0.443	0.007460±0.000947	0.006064±0.000806	0.029*
Thymus	0.004184±0.000449	0.005006±0.000690	0.056	0.003765±0.001312	0.005330±0.000898	0.051

Note: *indicates that the two sets of data were significantly different (P<0.05).

Table 3. Comparison of the organ coefficients of the two-month-old mice

	Hairless mice (♂)	Normal mice (♂)	*P*	Hairless mice (♀)	Normal mice (♀)	*P*
Heart	0.005248±0.000704	0.004994±0.000504	0.530	0.004636±0.000444	0.005176±0.000763	0.209
Liver	0.063626±0.003414	0.053298±0.001549	0.000*	0.060270±0.001804	0.049068±0.001672	0.000*
Spleen	0.004614±0.000543	0.00374±0.000385	0.019*	0.005502±0.000315	0.004626±0.000362	0.004*
Lung	0.004850±0.000648	0.004938±0.000378	0.800	0.005880±0.000471	0.005690±0.000205	0.432
Left kidney	0.009292±0.000785	0.007510±0.000786	0.007*	0.007360±0.000154	0.005888±0.000635	0.001*
Right kidney	0.008908±0.000753	0.007752±0.001005	0.074	0.007606±0.000959	0.006618±0.000676	0.096
Thymus	0.002142±0.000422	0.002442±0.000283	0.223	0.003382±0.000385	0.003626±0.0007128	0.520

Note: *indicates that the two sets of data were significantly different (*P*<0.05).

liver, spleen, lung, and kidney of the one-month-old male hairless mice were higher than those of the male normal mice, and the differences of the lung were significant. The average organ coefficients of heart, lung, and kidney of the one-month-old female hairless mice were higher than those of the female normal mice, and the differences of the heart, lung, and left kidney were significant. The average organ coefficients of the heart, liver, spleen, and kidney of the two-month-old male hairless mice were higher than those of the normal mice, and the differences in the coefficients of the liver, spleen, left kidney and right kidney were significant. The average organ coefficients of the liver, spleen, lung, and kidney of the two-month-old female hairless mice were higher than those of the normal mice, and the differences in the coefficients of the liver, spleen, and left kidney were significant. The average organ coefficient of the thymus of the NIH hairless mice was lower than that of the normal mice (**Tables 2**, **3**). Accordingly, the main differences in the organ coefficients between the NIH hairless mice and the normal mice were that the organ coefficients of most organs in the NIH hairless mice were high, while the organ coefficient of the thymus was low.

Histological observation of the organs and skin

The heart, liver, lung, kidney tissues of the NIH hairless mice and the normal mice showed no significant difference (**Figures 2**-**5**), whereas

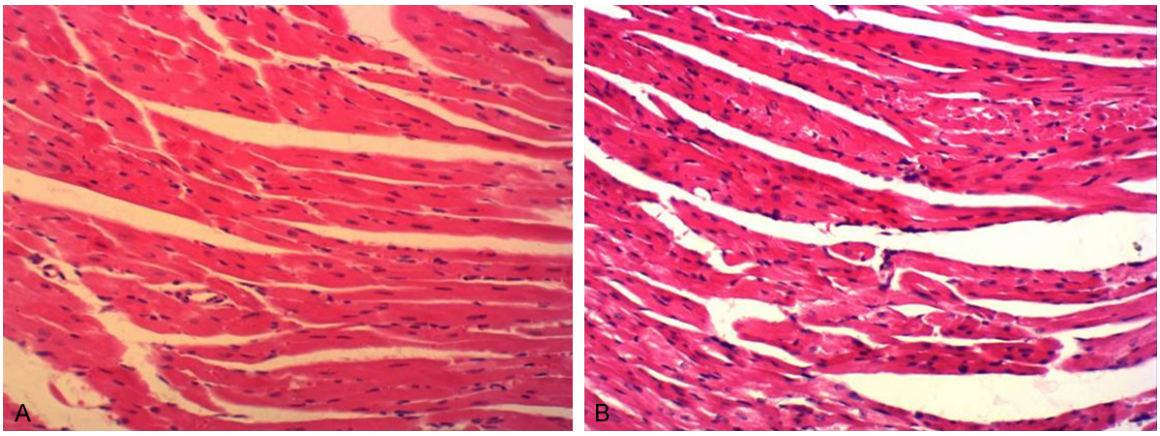

Figure 2. Sections of heart tissue for one-month-old mice (×200). A: NIH hairless mice; B: NIH normal mice. The cardiomyocytes of the NIH hairless mice are intact with no abnormalities.

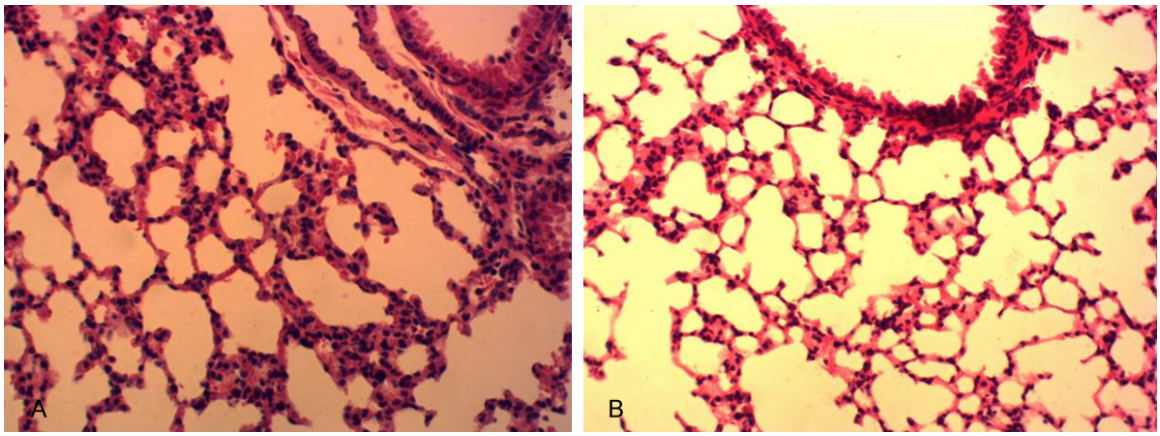

Figure 3. Sections of lung tissue for one-month-old mice (×200). A: NIH hairless mice; B: NIH normal mice. The lungs of the NIH hairless mice are clear with no hyperemia or septal thickening.

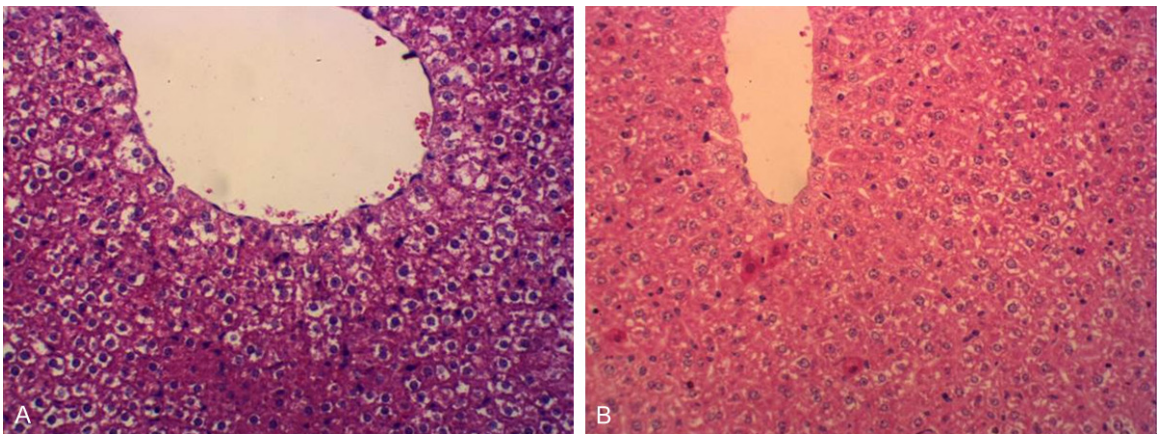

Figure 4. Sections of liver tissue for one-month-old mice (×200). A: NIH hairless mice; B: NIH normal mice. The stem cells of the NIH hairless mice were intact with a clear boundary, showing no significant inflammatory cell infiltration.

the structures of the skin were significantly different. The subcutaneous tissue and dermis of the NIH hairless mice had fewer follicles, with no obvious hair root and hair shaft, whereas

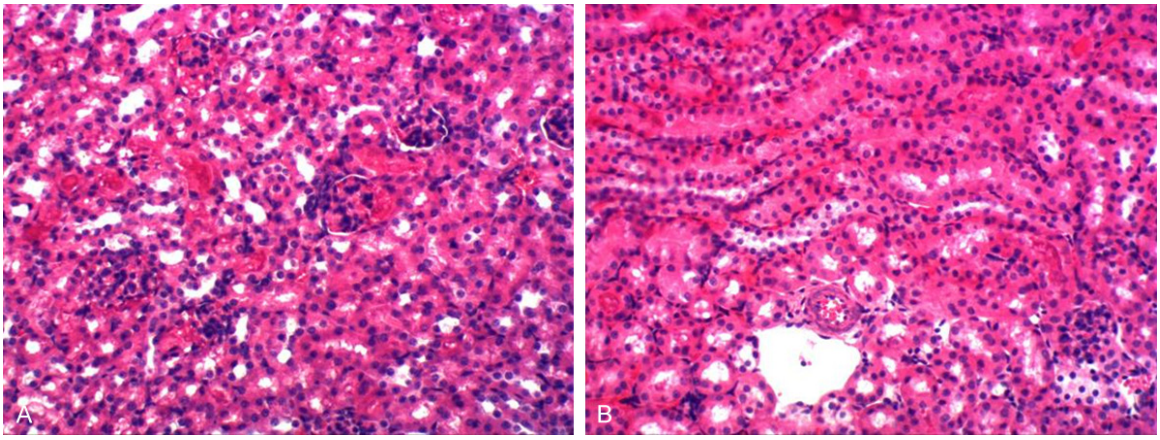

Figure 5. Sections of kidney tissue for one-month-old mice (×200). A: NIH hairless mice; B: NIH normal mice. The glomeruli of the NIH hairless mice showed no abnormalities, and the arrangements of the renal tubules were normal.

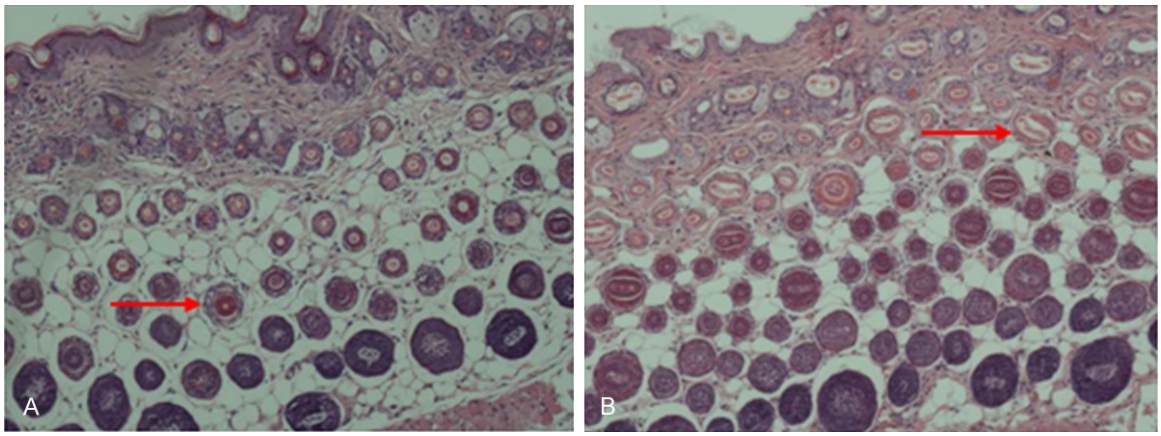

Figure 6. Sections of dorsal skin tissue for one-month-old mice (×200). (A) NIH hairless mice; (B) NIH normal mice. The number of follicles of the NIH hairless mice was significantly less than that of the normal mice; obvious hair shaft structures were not observed, and keratosis was found in the follicles. The → in (A) demonstrate the keratinized follicles, while the → in (B) show the shaft in the obvious hollow-like structures.

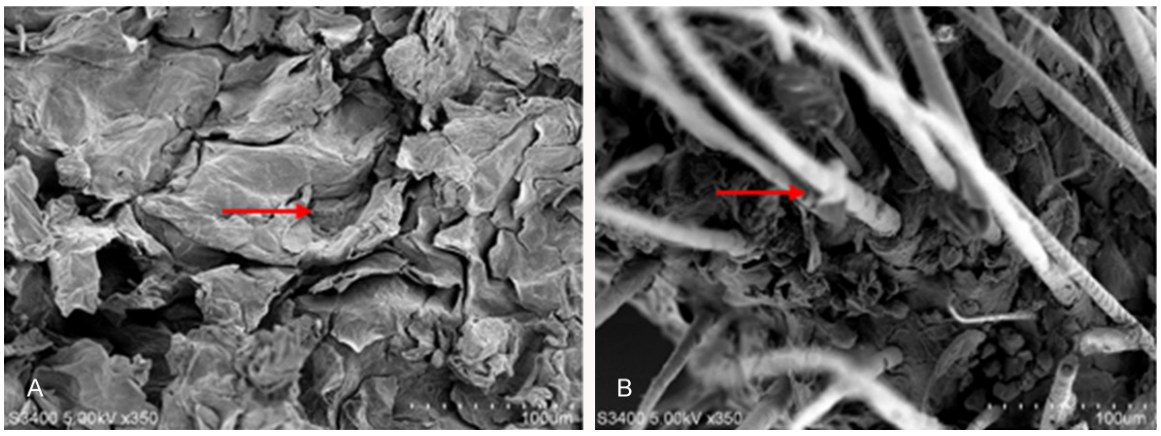

Figure 7. SEM images for the dorsal skin of the 7-day-old mice (×350 100 μm). A: The dorsal skin of a 7-day-old hairless mouse; no obvious hair growth was observed, and → demonstrates the keratinized layer-like substances; B: The dorsal skin of a 7-day-old normal mouse; → demonstrates the normally developed hair, and the dorsal skin was still observable.

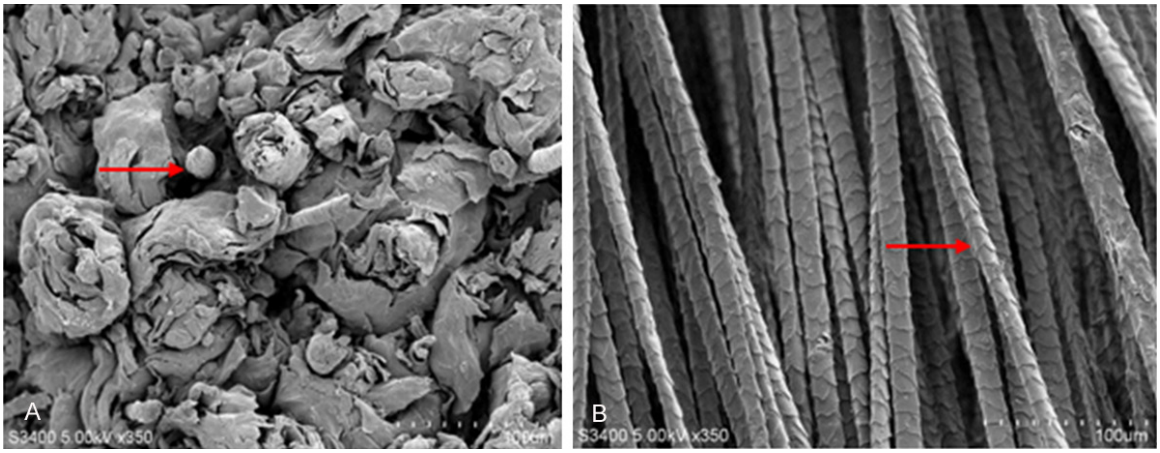

Figure 8. SEM images for the dorsal skin of the 14-day-old mice (×350 100 μm). A: The dorsal skin of a 14-day-old hairless mouse; → demonstrates the immature hair, with keratinized layer-like substances on the skin surface; B: The dorsal skin of a 14-day-old normal mouse; → demonstrates the normally developed hair, with a scaly surface in a regular arrangement. The dorsal skin was not observable.

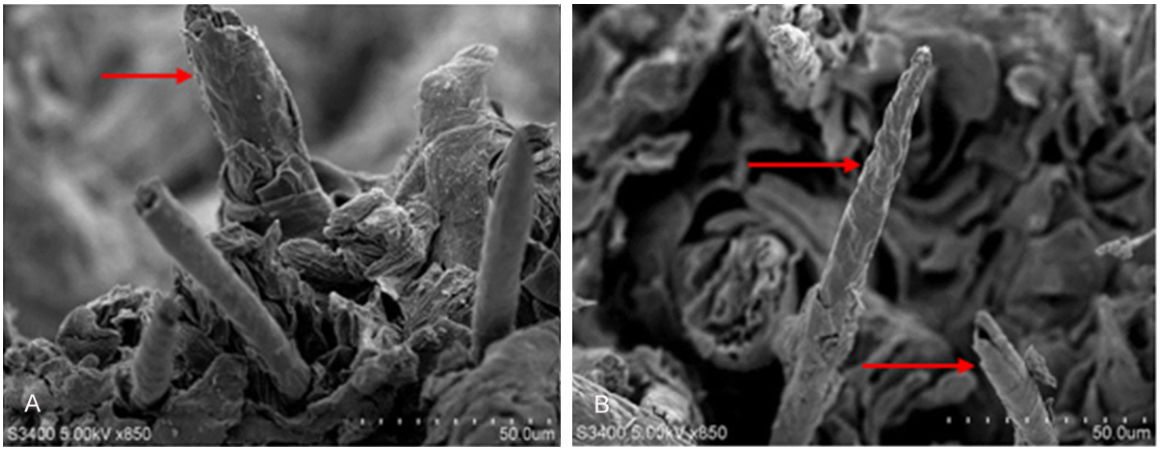

Figure 9. SEM images for the dorsal skin of a 14-day-old hairless mouse (×850 50 μm). With further magnification, incomplete hair growth can be observed at →; the scaly structure in a regular arrangement on the skin surface was not observed, and the front part of some hair even broke off.

hair shafts in a hollow-like structure could be observed in the normal mice (**Figure 6**).

Results of SEM for the dorsal skin

By SEM, growing hair can be clearly observed in the 7-day-old NIH normal mice, while almost no hair was growing in the 7-day-old NIH hairless mice, with the keratinized substances on the skin surface (**Figure 7**). The hair development in the 14-day-old NIH normal mice was normal, and the dorsal skin was not visible; in contrast, the hair development in the 14-day-old NIH hairless mice was incomplete, with extremely rare hair that showed defects in the hair structure (**Figures 8** and **9**).

Discussion

The litter size and survival rate of pups after weaning are two important indicators to measure the breeding ability of animals. The results of our statistical analysis showed that the litter size and the survival rate of pups after weaning of the NIH hairless mice were lower than those of the normal mice, indicating that the reproductive performance of the NIH hairless mice was poor. The female NIH hairless mice were able to fertilize and lactate, but the litter size and the survival rate of pups after weaning were relatively low. Many known mutations in the skin or hair affect the reproductive performance of mice. For example, neither male nor

female *at* mice are fertile; female *nu/nu* nude mice have no reproductive capacity; female hairless *hr/hr* mice have no lactating ability; female *mc* mice have no reproductive capacity; female *sf* mice are infertile; and female *ab* mice have reduced fertility [7]. Because of the poor reproductive performance of the NIH hairless mice, the reproductive capacity of the female mice will also decline with increasing age. Therefore, in the breeding process, healthy 2- to 3-month-old individual mice should be selected as the breeding mice.

The results of our statistical analysis showed that the main differences in the organ coefficients between the NIH hairless mice and the normal mice were that the organ coefficients of most organs in the NIH hairless mice were high, while the organ coefficient of the thymus was low. The light microscopy observations of the HE stained sections of the organ tissue demonstrated that the development of these organs in the NIH hairless mice was normal, with no significant abnormalities. Research has also shown that the hairless gene mutation not only affects the skin but also affects immune organs such as the thymus [8]. Zhang found that there is premature atrophy of the thymus in Yuyi hairless (YYHL) mice, leading to decreased immunity and a shortened life span in YYHL mice [9]. Autoimmune deficiency diseases were also observed in *sf* mice [10]. The organ coefficient of the thymus for the NIH hairless mice was low, suggesting that the thymus development of the NIH hairless mice may have defects, such as premature degradation.

The results of light microscopy observation showed that the number of follicles in the dorsal skin of the NIH hairless mice was less than that of the normal mice; further, keratosis occurred in the hair follicles, with no significant hair follicle structures. The SEM images illustrated that there was no hair growing on the skin surface of the 7-day-old NIH hairless mice, with keratinized layer-like substances on the skin surface. Although hair was observable on the skin surface in the 14-day-old mice, the hairs were significantly different compared to those of the normal mice, and the number of hair was very low. Zhu and Zhang observed a similar phenomena in YYHL mice [9, 11]; Wu also made similar observations in snthr-^{1bao} hairless mice [12]. Development of hair is closely related to the development of hair follicles, and abnormalities in follicle development will directly affect hair development. For example, the *sa* gene has a direct impact on the hair bulb to affect the hair growth, resulting in the satin hair phenotype in mice [13, 14]. Currently, the hyperkeratosis in the hair follicles of the NIH hairless mice is speculated as the exact reason for the failure of normal hair growth, and whether the hyperkeratosis of follicles will become more severe with increasing age is not clear yet.

To date, more than 140 genes affecting the coating and the structure of hair have been reported, of which the *hr* gene is the one attracting the most research interest. The *hr* gene plays an irreplaceable role in catagen, and deficiency in the *hr* gene function can prevent successful hair growth [15]. In the mutant mice carrying the hairless gene and its allele, their hair structure changed, and their thymus also showed structural changes of accelerated degeneration with age [16]. As a member of the family of the winged helix/forkhead transcription factors, the *Foxn1* gene is expressed in skin and TECs. Studies have shown that the *Foxn1* gene plays a key role in the early development of thymus and skin; the deletion of *Foxn1* genes also affected the normal development of thymus and skin [17]. Cunliffe VT confirmed that the *nu* mice phenotype is caused by a mutation in the *Foxn1* gene [18]. Identifying the mutations causing the phenotype of the NIH hairless mice may contribute to further investigations of the NIH hairless mice model.

Gene mutations include spontaneous mutations and induced mutations, and valuable animal models can be obtained by these two approaches. Zhang Jintao found mice that lose their hair in the breeding process of KM mice and successfully reproduced and established the inbred strain of YYHL mice. Mao obtained two new strains of hairless mice by ENU mutagenesis. Li SR also established *Uncv* mice in the breeding process of BALB/c mice [19]. These mice with the obtained mutated gene showed differences from normal mice in not only skin and coat development but also reproductive performance and histological characteristics [20, 21]. Spontaneous mutations in mice are those mutations that are naturally occurring in the breeding process of mice; they

represent an important approach to acquiring new genetic variations and gene functions with a very low probability [22]. As a type of new mutant mice with a spontaneous mutation that affects the coat, the NIH hairless mice obtained in our laboratory showed significant differences from the NIH normal mice not only in the hair development on the skin surface but also in the reproductive performance and histological characteristics. Thus, these mice have great potential to be developed as a new animal model.

Acknowledgements

National Key Technology R&D Program (2015BAI07B02 and 20150101102JC), National Natural Science Foundation of China (31501954).

Disclosure of conflict of interest

None.

Address correspondence to: Drs. Jia-Bao Zhang and Wen-Zhi Ren, Department of College of Animal Sciences, Jilin University, No. 5333, Xi'an Road, Changchun 130062, China. Tel: +86 431 87836551; Fax: +86 431 87836551; E-mail: zjb515@126.com (JBZ); rwz1964@163.com (WZR)

References

[1] Qin B, Tu C, Zhang B, He T, Fu L and Xu W. A modified murine model based on hydrodynamic injection for the analysis of chronic human hepatitis B virus infection. Mol Med Rep 2013; 8: 1677-1682.

[2] Pirog KA, Irman A, Young S, Halai P, Bell PA, Boot-Handford RP and Briggs MD. Abnormal chondrocyte apoptosis in the cartilage growth plate is influenced by genetic background and deletion of CHOP in a targeted mouse model of pseudoachondroplasia. PLoS One 2014; 9: e85145.

[3] Lorenz J, Seebach E, Hackmayer G, Greth C, Bauer RJ, Kleinschmidt K, Bettenworth D, Bohm M, Grifka J and Grassel S. Melanocortin 1 receptor-signaling deficiency results in an articular cartilage phenotype and accelerates pathogenesis of surgically induced murine osteoarthritis. PLoS One 2014; 9: e105858.

[4] Jo DH, Lee JH, Jun HJ, Kim J, Wen Q, Hoang MH, Yu YS, Kim JH and Lee SJ. Gene expression profiles of primary retinal pigment epithelial cells from apolipoprotein E knockout and human apolipoprotein E2 transgenic mice. Genet Mol Res 2015; 14: 1855-1867.

[5] Han D, Yao Y, Sun Y, Gong Y and Wu X. Effect of charred Radix et Rhizoma Rhei in a laser-induced choroidal neovascularization murine model. Mol Med Rep 2015; 11: 2896-2902.

[6] Kim JI, Park S, Lee S, Lee I, Heo J, Hwang MW, Bae JY, Kim D, Jang SI, Park MS and Park MS. DBA/2 mouse as an animal model for anti-influenza drug efficacy evaluation. J Microbiol 2013; 51: 866-871.

[7] Joseph LB, Heck DE, Cervelli JA, Composto GM, Babin MC, Casillas RP, Sinko PJ, Gerecke DR, Laskin DL and Laskin JD. Structural changes in hair follicles and sebaceous glands of hairless mice following exposure to sulfur mustard. Exp Mol Pathol 2014; 96: 316-327.

[8] San JI, Garcia-Suarez O, Hannestad J, Cabo R, Gauna L, Represa J and Vega JA. The thymus of the hairless rhino-j (hr/rh-j) mice. J Anat 2001; 198: 399-406.

[9] Zhang JT, Fang SG and Wang CY. A novel nonsense mutation and polymorphisms in the mouse hairless gene. J Invest Dermatol 2005; 124: 1200-1205.

[10] Kasprowicz DJ, Smallwood PS, Tyznik AJ and Ziegler SF. Scurfin (FoxP3) controls T-dependent immune responses in vivo through regulation of CD4+ T cell effector function. J Immunol 2003; 171: 1216-1223.

[11] Zhang JT, Wang CY, Kang QZ, Du XT and Xue JL. Establishment of segregating inbred strain of Yuyi hairless mice and its monitoring of genetic characteristics. Yi Chuan Xue Bao 2002; 29: 221-225.

[12] Wu BJ, Shao YX, Mao HH, Tang D, Liu J, Xue ZF and Li HD. Two kinds of ENU-induced scant hair mice and mapping of the mutant genes. J Dermatol Sci 2004; 36: 149-156.

[13] Lee CW, Ko HH, Lin CC, Chai CY, Chen WT and Yen FL. Artocarpin attenuates ultraviolet B-induced skin damage in hairless mice by antioxidant and anti-inflammatory effect. Food Chem Toxicol 2013; 60: 123-129.

[14] Potter CS, Peterson RL, Barth JL, Pruett ND, Jacobs DF, Kern MJ, Argraves WS, Sundberg JP and Awgulewitsch A. Evidence that the satin hair mutant gene Foxq1 is among multiple and functionally diverse regulatory targets for Hoxc13 during hair follicle differentiation. J Biol Chem 2006; 281: 29245-29255.

[15] Panteleyev AA, Paus R and Christiano AM. Patterns of hairless (hr) gene expression in mouse hair follicle morphogenesis and cycling. Am J Pathol 2000; 157: 1071-1079.

[16] Smee DF, Bailey KW, Wong MH and Tarbet EB. Topical treatment of cutaneous vaccinia virus infections in immunosuppressed hairless mice with selected antiviral substances. Antivir Chem Chemother 2011; 21: 201-208.

[17] Palamaro L, Romano R, Fusco A, Giardino G, Gallo V and Pignata C. FOXN1 in organ development and human diseases. Int Rev Immunol 2014; 33: 83-93.

[18] Cunliffe VT, Furley AJ and Keenan D. Complete rescue of the nude mutant phenotype by a wild-type Foxn1 transgene. Mamm Genome 2002; 13: 245-252.
[19] Li SR, Wang DP, Yu XL, Ge BS, Wang CE, Lu YF, Li JQ, Wu N, Li RF, Zhu SE, Zhang ZC and Chen YF. Uncv (uncovered): a new mutation causing hairloss on mouse chromosome 11. Genet Res 1999; 73: 233-238.
[20] Tharmarajah G, Faas L, Reiss K, Saftig P, Young A and Van Raamsdonk CD. Adam10 haploinsufficiency causes freckle-like macules in Hairless mice. Pigment Cell Melanoma Res 2012; 25: 555-565.
[21] Lim JY, Kim OK, Lee J, Lee MJ, Kang N and Hwang JK. Protective effect of the standardized green tea seed extract on UVB-induced skin photoaging in hairless mice. Nutr Res Pract 2014; 8: 398-403.
[22] Jain AK, Tewari-Singh N, Inturi S, Orlicky DJ, White CW and Agarwal R. Histopathological and immunohistochemical evaluation of nitrogen mustard-induced cutaneous effects in SKH-1 hairless and C57BL/6 mice. Exp Toxicol Pathol 2014; 66: 129-138.